Polymer 53 (2012) 1219–1228

Contents lists available at SciVerse ScienceDirect

Polymer

journal homepage: www.elsevier.com/locate/polymer

# Enhancement of photovoltaic properties in supramolecular polymer networks featuring a solar cell main-chain polymer H-bonded with conjugated cross-linkers

Dhananjaya Patra [a], Mohan Ramesh [a], Duryodhan Sahu [a], Harihara Padhy [a], Chih-Wei Chu [b,c,**], Kung-Hwa Wei [a], Hong-Cheu Lin [a,*]

[a] Department of Materials Science and Engineering, National Chiao Tung University, 1001 Ta Hsueh Road, Hsinchu 30049, Taiwan, ROC
[b] Research Center for Applied Sciences, Academia Sinica, Taipei, Taiwan, ROC
[c] Department of Photonics, National Chiao Tung University, Hsinchu, Taiwan, ROC

ARTICLE INFO

*Article history:*
Received 9 November 2011
Received in revised form
12 January 2012
Accepted 15 January 2012
Available online 2 February 2012

*Keywords:*
H-bonded cross-linker
Supramolecule
Polymer network

ABSTRACT

Stille polymerization was employed to synthesize a low-band-gap (LBG) conjugated main-chain polymer **PBTH** consisting of bithiazole, dithieno[3,2-b:2′,3′-d]pyrroles (DTP), and pendent melamine derivatives. Novel supramolecular polymer networks **PBTH/C** and **PBTH/F** were developed by mixing proper molar amounts of polymer **PBTH** (containing melamine pendants) to be hydrogen-bonded (H-bonded) with complementary uracil-based conjugated cross-linkers **C** and **F** (i.e., containing two symmetrical uracil moieties connected with carbazole and fluorene units through triple bonds). The formation of multiple H-bonds between polymer **PBTH** and cross-linkers **C** or **F** was confirmed by FT-IR measurements. In contrast to polymer **PBTH**, the supramolecular design with multiple H-bonds can enhance the photovoltaic properties of polymer solar cell (PSC) devices containing H-bonded polymer networks **PBTH/C** and **PBTH/F** by tuning their light harvesting capabilities, HOMO energy levels, and crystallinities. Initially, the power conversion efficiency (PCE) values of PSC devices containing supramolecular polymer networks **PBTH/C** and **PBTH/F** as electron donors and [6,6]-phenyl-$C_{71}$-butyric acid methyl ester ($PC_{70}BM$) as an electron acceptor (polymer:$PC_{70}BM$ = 1:1 w/w) are found to be 0.97 and 0.68%, respectively, in contrast to 0.52% for polymer **PBTH**. The highest PCE value of 1.56% with a short-circuit current densities ($J_{sc}$) value of 7.16 mA/cm$^2$, a open circuit voltages ($V_{oc}$) value of 0.60 V, and a fill factor (FF) of 0.36 was further optimized in the PSC device containing a supramolecular polymer network **PBTH/C** as polymer:$PC_{70}BM$ = 1:2 w/w. These results indicate that supramolecular design is an effective route towards better photovoltaic properties of $V_{oc}$, $J_{sc}$, and PCE values in polymer solar cells.



## 1. Introduction

Over the past decade, exploiting and tailoring novel materials with promoted properties by utilizing supramolecular approaches in conjunction with π-conjugated structures is one of the key way to design optoelectronic devices [1].Control of hierarchical self-assembled behaviors of various π-conjugated molecules through multiple hydrogen bonds can generate nano-structural materials with long-range orders intrinsically, in which defect-free structures are feasible to be the bottom-up approach via supramolecular chemistry [2]. Due to self-assembly between complementary molecular components, a variety of non-covalent interactions, for instance hydrogen bonds (H-bonds) [3,4], ionic forces [5], and metal-coordinations [6], can produce unique properties, which are not possessed by the individual components. Among these supramolecular interactions, H-bonds are ideal non-covalent interactions to form self-assembled architectures due to their selectivity and directionality [1c]. Tremendous research efforts have been devoted towards engineering of polymeric materials as well as donor-acceptor (D-A) bulk heterojunction (BHJ) solar cell devices due to substantial future prospects as low-cost 3rd generation photovoltaic technology [7]. Remarkable achievements in the field of conjugated polymers and dramatic increase in device performance, reaching a power conversion efficiencies (PCE) over 7% by utilizing low-band-gap (LBG) polymers as electron donors and fullerene derivatives, such as [6,6]-phenyl-$C_{61}$-butyric acid methyl ester ($PC_{61}BM$) or [6,6]-phenyl-$C_{71}$-butyric acid methyl ester ($PC_{70}BM$), as electron acceptors [8].

* Corresponding author. Tel.: +886 3 5712121; fax: +886 3 5724727.
** Corresponding author. Research Center for Applied Sciences, Academia Sinica, Taipei, Taiwan, ROC.
*E-mail addresses:* gchu@gate.sinica.edu.tw (C.-W. Chu), linhc@cc.nctu.edu.tw (H.-C. Lin).

0032-3861/$ – see front matter © 2012 Elsevier Ltd. All rights reserved.
doi:10.1016/j.polymer.2012.01.026

An enhanced intermolecular π-stacking, long-range order, and solution processable electron-donating dithieno[3,2-b:2′,3′-d] pyrroles (DTP) unit can be co-polymerized with various electron-deficient units to generate LBG polymers and showed PCE values up to ~3% [9]. However, due to high values of the highest occupied molecular orbital (HOMO) levels in DTP-based polymers, they showed relatively low $V_{oc}$ values and thus to result in low PCE values for organic solar cells [10]. This problem can be solved either by using various electron-deficient units [10,11a] or introducing supramolecular architectures to manipulate their HOMO energy levels and thus to get higher $V_{oc}$ values. As an electron-deficient unit, the bithiazole unit containing two electron-withdrawing imine (−C=N) could show high oxidative stabilities and minimize the HOMO energy levels to induce the high $V_{oc}$ values [10,11a]. However, Li et al. have reported one D-A copolymer containing DTP and bithiazole sandwiched between two thiophene units only possessed a maximum PCE value of 0.06% [9b], but our later report demonstrated that one of the analogous D-A copolymers containing DTP, thiophene, and bithiazole units could reach a maximum PCE value of 0.69% [10b].

The design of supramolecular D-A systems was recognized as a promising strategy via the charge-transfer processes between donor and acceptor units [4]. Würthner, Schenning, and Meijer et al. reported well-defined mesoscopic assemblies by using complementary H-bonded moieties of perylene bisimide and melamine derivatives [4,12]. Moreover, Bonifazi and Samori et al. constructed several discrete and multi-component nano-scale supramolecular assemblies from triple H-bonded D-A complexes consisting of diamino-pyridine and uracil derivatives [1b,13]. In addition, Meijer et al. reported a PCE value of 0.39% for the polymer solar cell (PSC) device by utilizing a main-chain H-bonded polymer containing oligo(p-phenylene vinyene) and ureido-pyrimidinone units (as H-bonded groups) [14]. Small molecules and their polymer analogues have attracted exceptional attentions in the recent days owing to their corresponding advantages, including high purities and (hole and electron) mobilities for small molecules, and easy processing capabilities and low costs for polymers. Consequently [15], one of the attractive approaches is to achieve advanced π-conjugated materials by the combination of both small molecular and polymeric designs through supramolecular architectures, so the H-bonded polymer networks are explored in this report. Our previous studies focus on solar cell dyes H-bonded to conjugated side-chain polymers to form either supramolecular side-chain polymers by single H-bonds attached to one side of (asymmetric) single carboxylic acid dyes [16a] or supramolecular polymer networks by single H-bonds attached to both sides of (symmetric) double carboxylic acid dyes [16b]. However, these proton acceptor polymers contain pyridyl pendants to form weak single H-bonds, and have shorter conjugation to exhibit worse solar cell properties than the conjugated main-chain polymers. Therefore, a conjugated main-chain polymer (with better PSC properties) containing multiple H-bonded pendants (with stronger H-bonds to the π-conjugated small molecules) is applied to our molecular design of supramolecular architectures in this study.

To the best of our knowledge, it is the first time to disclose the supramolecular polymer networks containing multiple functionalized melamine pendants and complementary H-bonded uracil motifs for the PSC applications. To accomplish this goal, we choose DTP, bithiazole, and thiophene units as the backbone of a conjugated main-chain polymer **PBTH**, in which the melamine pendants can be H-bonded with complementary uracil-based conjugated cross-linkers **C** and **F** (in proper molar amounts), i.e., the symmetrical uracils of cross-linkers **C** and **F** are linked to central carbazole and fluorene units, respectively, through triple bonds (see Fig. 1.), to generate supramolecular polymer networks **PBTH/C** and **PBTH/F**. The unique features of this triple H-bonded approach are to tune light harvesting capabilities, manipulation of HOMO energy levels, and power conversion efficiencies of supramolecular polymer networks **PBTH/C** and **PBTH/F**. Moreover, the functionalized supramolecular polymer networks are developed to possess better solubilities as well as processabilities in solvents and enhance photovoltaic properties in this study.

## 2. Experimental

### 2.1. Materials

All chemicals and solvents were reagent grades and purchased from Aldrich, ACROS, Fluka, and Lancaster and $Pd(PPh_2)Cl_2$ and $Pd(PPh_3)_4$ recived from Stream Chemical Co. Tetrahydrofuran (THF), toluene, and diethyl ether were distilled over sodium/benzophenone. Absolute ethanol was obtained by refluxing with magnesium ethoxide and then distilled. The other reagents were used as received without further purification.

### 2.2. Measurements and characterization

$^1H$ and $^{13}C$ NMR spectra were recorded on a Varian Unity 300 MHz spectrometer using $CDCl_3$ solvent, "br" was noted for broad peaks and chemical shifts were reported as $\delta$ values (ppm) relative to an internal tetramethylsilane (TMS) standard. Elemental analyses were performed on a HERAEUS CHN-OS RAPID elemental analyzer. Thermogravimetric analyses were conducted with a TA Instruments Q500 at a heating rate of 10 °C/min under nitrogen. Gel permeation chromatography (GPC) analyses were conducted on a Waters 1515 separation module using polystyrene as a standard and THF as an eluant. UV−visible absorption spectra were recorded in dilute dichlorobenzene solutions and solid films (spin-coated on glass substrates from dichlorobenzene solutions) on an HP G1103A spectrophotometer. Cyclic voltammetry (CV) measurements were performed at a scanning rate of 100 mV/s at room temperature using a BAS 100 electrochemical analyzer with a standard three-electrode electrochemical cell in 0.1 M tetrabutylammonium hexafluorophosphate ($TBAPF_6$) solution in acetonitrile. During the CV measurements, the solutions were purged with nitrogen for 30 s. In each case, a carbon rod coated with a thin layer of polymers as the working electrode, a platinum wire as the counter electrode, and a silver wire as the quasi-reference electrode were used, and Ag/AgCl (3M KCl) electrode was served as a reference electrode for all potentials quoted herein. The redox couple of ferrocene/ferocenium ion ($Fc/Fc^+$) was used as an external standard. The corresponding highest occupied molecular orbital (HOMO) was calculated using $E_{ox/onset}$ for experiment in solid film of polymer, which were performed by drop-casting film with the similar thickness from THF solutions (ca. 5 mg/ml). The LUMO level of PCBM employed was in accordance with the literature data [17]. The onset potentials were determined from the intersections of two tangents drawn at the rising currents and background currents of the CV measurements.

### 2.3. Fabrication and testing of polymer solar cells

The polymer photovoltaic cells in this study contained an active layer of polymer **PBTH**, supramolecular polymer networks **PBTH/C** and **PBTH/F** blended with $PC_{70}BM$ in solid films, which was sandwiched between a transparent indium tin oxide (ITO) anode and a metal cathode (Ca). Prior to the device fabrication, ITO-coated glass substrates (1.5 × 1.5 $cm^2$) were ultrasonically cleaned in detergent, deionized water, acetone, and isopropyl alcohol. After routine solvent cleaning, the substrates were treated with UV ozone for 20 min. Then, a modified ITO surface was obtained by

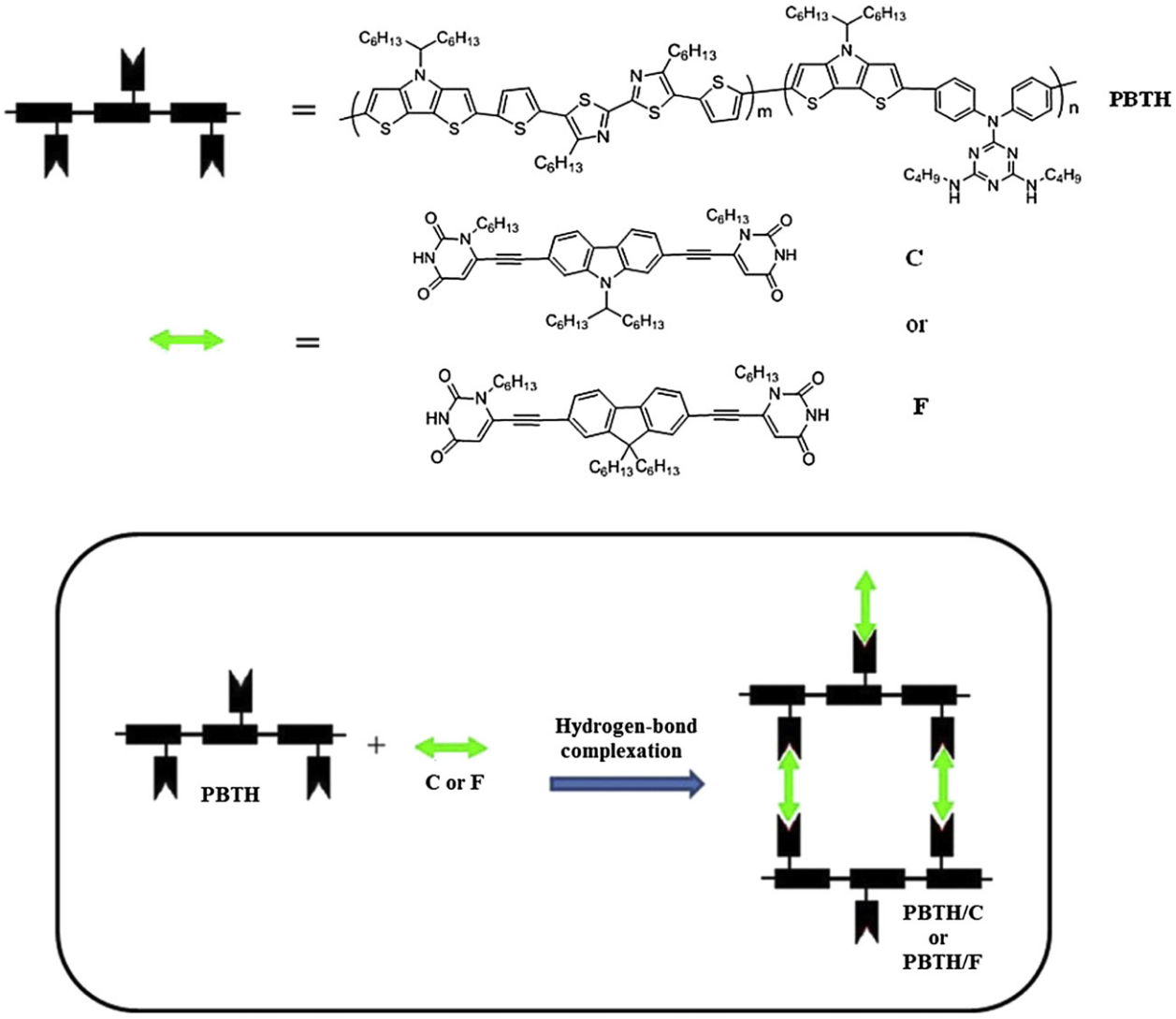


**Fig. 1.** Schematic illustration of conjugated main-chain polymer (**PBTH**) and supramolecular polymer networks (**PBTH/C**, and **PBTH/F**).

spin-coating a layer of poly(ethylene dioxythiophene):polystyrenesulfonate (PEDOT:PSS) (~30 nm). After thermal treating at 130 °C for 1 h, the substrates were transferred to a nitrogen-filled glove box. Subsequently, on the top of PEDOT:PSS layer, the active layer was prepared by spin coating from blended solutions of **PBTH**, **PBTH/C** and **PBTH/F**: $PC_{70}BM$ (with 1:1 w/w) with a spin rate ca. 1000 rpm, and the thickness of the active layer was typically ca. 90 nm. Initially, the blended solutions were prepared by dissolving both polymers and $PC_{70}BM$ in chlorobenzene (10 mg/1 ml), followed by continuous stirring for 12 h at 50 °C. In the slow-growth approach, blended polymers in solid films were kept in the liquid phase after spin-coating by using the solvent with a high boiling point (such as chlorobenzene) and allowed to dry the solvent slowly. Finally, a calcium layer (30 nm) and a subsequent aluminum layer (100 nm) were thermally evaporated through a shadow mask at a pressure below $6 \times 10^{-6}$ Torr to have the active device area of 0.12 $cm^2$. All PSC devices were prepared and measured under ambient conditions. The solar cell testing was done inside a glove box under simulated AM 1.5G irradiation (100 $mW/cm^2$) using a Xenon lamp based solar simulator (Thermal Oriel 1000 W). The light intensity was calibrated by a mono-silicon photodiode with KG-5 color filter (Hamamatsu).

### *2.4. Synthesis of monomer **M1**, conjugated cross-linkers (**C** and **F**), and conjugated main-chain polymer **PBTH***

#### *2.4.1. 4,6-Dichloro-N,N-diphenyl-1,3,5-triazin-2-amine (**1**)*

Under $N_2$, a solution of diphenylamine (9.16 g, 54.22 mmol) in THF (50 ml) was added dropwise to a mixture of diisopropylethylamine (9.5 ml, 54.22 mmol) and 2,4,6-trichloro-1,3,5-triazine (10.0 g, 52.22 mmol) in THF(150 ml) at 20 °C. After stirring for 3 h, the solvent was removed by rotatary evaporatior and the residue was purified by column chromatography (hexane: ethyl acetate = 4:1) to give a white color solid. (12.9 g, yield 75%). $^1H$ NMR (300 MHz, $CDCl_3$, $\delta$): 7.45–7.41 (m, 4H), 7.35–7.33 (m, 2H), 7.30–7.27 (m, 4H). $^{13}C$ NMR (75 MHz, $CDCl_3$, $\delta$): 170.83, 166.06, 141.81, 129.73, 127.91, 127.40.

#### *2.4.2. $N^2$,$N^4$-dibutyl-$N^6$,$N^6$-diphenyl-1,3,5-triazine-2,4,6-triamine (**2**)*

Sodium bicarbonate (8.0 g, 84.01 mmol) was added to a solution of compound **1** (10.0 g, 31.52 mmol) in 1,4-dioaxane (100 ml). After that, butyl amine (9.4 ml, 94.58 mmol) was added and the resulting mixture was refluxed overnight. The reaction mixtures was cooled to room temperature and pour into cold water and extracted three

times with ethyl acetate. The combined organic fractions were washed with brine, dried over magnesium sulphate ($MgSO_4$), and concentrated by rotary evaporation and purified by column chromatography, (hexane: ethyl acetate = 7:3) to give a white solid. (10.70 g, yield 87%). $^1$H NMR (300 MHz, $CDCl_3$, $\delta$):7.45–7.41 (m, 4H), 7.35–7.33 (m, 2H), 7.30–7.27 (m, 4H),4.84 (br, 2H), 3.34–3.11(br, 4H), 1.43–1.25 (m, 8H), 0.88 (t, $J$ = 6.2 Hz, 6H). $^{13}$C NMR (75 MHz, $CDCl_3$, $\delta$): 166.49, 144.61, 128.62, 128.28, 125.28, 40.57, 32.15, 20.25, 14.03.

### 2.4.3. $N^2$,$N^2$-bis(4-bromophenyl)-$N^4$,$N^6$-dibutyl-1,3,5-triazine-2,4,6-triamine (**M1**)

*N*-Bromosuccinimide (NBS) (6.9 g, 38.40 mmol) was added portion-wise to a solution of compound **2** (5.0 g, 12.80 mmol) in af (50 ml) at 0 °C. The reaction mixture was stirred for 6 h at the same temperature and water was added to quench the reaction. The organic layer was extracted three times by ethyl acetate followed by brine and water washing and dried over anhydrous $MgSO_4$. The solvent was removed by rotary evaporator and the product was further purified by column chromatography (hexane: ethyl acetate = 4:1) to yield a white solid. (5.7 g, 80%). $^1$H NMR (300 MHz, $CDCl_3$, $\delta$): 7.47–7.38 (m, 4H), 7.43–7.28 (m, 4H), 4.84 (br, 2H), 3.34–3.31(br, 4H), 1.43–1.25 (m, 8H), 0.88 (t, $J$ = 6.2 Hz, 6H). $^{13}$C NMR (75 MHz, $CDCl_3$, $\delta$): 166.48, 166.11, 143.25, 131.81, 129.77, 118.79, 40.60, 32.09, 20.24, 14.01; EIMS [$M^+$] calcd. m/z = 548.32, found 548.0. Anal. Calcd. for $C_{23}H_{28}Br_2N_6$: C, 50.38; H, 5.15; Br, 29.15; N, 15.33; found: C, 50.78; H, 5.48; N, 15.04.

### 2.4.4. 1-Hexyluracil (**3**)

Potassium carbonate ($K_2CO_3$) (14.80 g, 107.05 mmol) was added to a suspension of uracil (10.0 g, 89.21 mmol) in dimethyl sulfoxide (DMSO) (150 ml), and stirred for 15–20 min at 45 °C. 1-Bromohexane (3.5 ml, 25 mmol) was added and the reaction mixture was stirred for 48 h. The reaction was cooled to room temperature and poured into cold water. The product was extracted three times with dichloromethane (DCM), and washed with dilute HCl, water, brine, and dried over $MgSO_4$. The organic layer was concentrated and poured into cold hexane with vigorous stirring. The resulting precipitate was filtered and washed with cold hexane to afford compound **3** (12.40 g, 70.9%) as a white solid. $^1$H NMR (300 MHz, $CDCl_3$, $\delta$): 9.12 (br, 1H), 7.14 (d, $J$ = 9.0 Hz, 1H), 5.70 (d, $J$ = 6.0 Hz, 1H), 3.71(t, $J$ = 7.5 Hz, 2H), 1.74–1.65 (m, 2H), 1.34–1.27 (m, 6H), 0.88 (t, $J$ = 6.6 Hz, 3H).$^{13}$C NMR (75 MHz, $CDCl_3$, $\delta$): 165.24; 150.55; 144.80; 100.75; 48.67; 31.79; 28.26; 25.61; 22.48; 13.91.

### 2.4.5. 1-Hexyl-6-iodouracil (**4**)

At −78 °C, lithium diisopropylamide (LDA) (20.4 ml of a 2.5 M solution, 51.0 mmol) was added drop-wise to a solution of 1-hexyluracil (2.0 g, 10.2 mmol) in THF (55 ml), and the resulting solution was stirred under $N_2$ for 2 h. $I_2$ (12.9 g, 51.0 mmol) was added and the reaction mixture was stirred for another 2 h at the same temperature. Acetic acid (2.0 ml) was added under stirring at room temperature overnight. The organic phase was extracted with ethyl acetate, washed with saturated $NaHCO_3$ (3 × 30.0 ml) and $Na_2SO_3$ (3 × 30 ml) solutions. Finally, the product was washed with brine (30 ml), and dried over $MgSO_4$. The solvent was removed by rotary evaporator and the crude product was purified by column chromatography (hexane: ethyl acetate = 5:5) to afford compound **4** (2.2 g, 67%). $^1$H NMR (300 MHz, $CDCl_3$, $\delta$): 9.48 (br, 1H), 6.41 (s, 1H), 4.0 (t, $J$ = 8.1 Hz, 2H), 1.74–1.65 (m, 2H), 1.34–1.27 (m, 6H), 0.88 (t, $J$ = 6.9 Hz, 3H).$^{13}$C NMR (75 MHz, $CDCl_3$, $\delta$): 160.65; 148.19; 115.91; 113.52; 53.48; 31.36; 27.45; 26.32; 22.17; 14.18.

### 2.4.6. 4,4′-(9-(Tridecan-7-yl)-9H-carbazole-2,7-diyl)bis(2-methylbut-3-yn-2-ol) (**6**)

To a solution of 2,7-dibromo-9-(tridecan-7-yl)-9*H*-carbazole (5) (5.0 g, 9.84 mmol) in 50 ml of THF/$Et_3N$ (1/1), 3-methyl-1-butyn-3-ol (3.85 ml, 39.37 mmol), $Pd(PPh_3)_2Cl_2$ (0.13 g, 0.28 mol), $PPh_3$ (0.1 g, 0.39 mol), and CuI (0.07 g, 0.39 mmol) were added. The reaction mixture was degassed with nitrogen for 30 min, and refluxed at 70 °C under $N_2$ for 12 h. The solvent was removed under reduced pressure and resulting solid was extracted with DCM then dried over $MgSO_4$. The crude product was purified by column chromatograph (hexane: ethyl acetate = 4:1) to afford a white solid (3.9 g, 77%). $^1$H NMR (300 MHz, $CDCl_3$, $\delta$): 7.97 (t, $J$ = 9.0, 2H), 7.65 (s, 1H), 7.47 (s, 1H), 7.30 (m, 2H), 4.48 (m, 1H), 2.29–2.17 (m, 2H), 1.95–1.87 (m, 2H), 1.67 (s, 12H), 1.28–0.1.08 (m, 16H), 0.80 (t, $J$ = 6.6 Hz, 6H).$^{13}$C NMR (75 MHz, $CDCl_3$, $\delta$): 144.42, 131.05, 130.49, 124.29, 117.02, 115.25, 93.91, 84.23, 81.55, 65.88, 65.78, 47.83, 33. 80, 31.81, 29.20, 27.10, 22.70, 14.20.

### 2.4.7. 2,7-Diethynyl-9-(tridecan-7-yl)-9H-carbazole (**7**)

A mixture of compound **6** (3.5 g, 6.81 mmol) and KOH (2.70 mg, 47.68 mmol) in 60 ml of 2-propanol was heated to reflux under $N_2$ with a vigorous stirring for 4 h. Solvent was removed and then the crude product was purified by column chromatography (hexane) to afford a white solid (1.90 g, 70%). $^1$H NMR (300 MHz, $CDCl_3$, $\delta$): 8.01 (t, $J$ = 9.0, 2H), 7.72 (s, 1H), 7.56 (s, 1H), 7.35 (d, 2H), 4.48 (m, 1H), 3.15 (s, 1H), 2.30–2.17 (m, 2H), 1.97–1.87 (m, 2H), 1.25–1.04 (m, 16H), 0.80 (t, $J$ = 6.6 Hz, 6H). $^{13}$C NMR (75 MHz, $CDCl_3$, $\delta$): 142.27, 138.43, 124.08, 123.21, 122.65, 120.82, 119.58, 115.67, 113.18, 85.27, 57.10, 33.89, 31.78, 29.25, 27.02, 22.73, 14.19.

### 2.4.8. 6,6′-(9-(Tridecan-7-yl)-9H-carbazole-2,7-diyl)bis(ethyne-2,1-diyl)bis(1-hexylpyrimidine-2,4(1H,3H)-dione) (**C**)

To a mixture of compound **7** (0.5 g, 1.26 mmol) in 20 ml THF/$NEt_3$ (1:1), compound **4** (1.22 g, 3.77 mmol), triphenylphosphine (13 mg, 0.05), and CuI (10 mg, 0.05 mmol) were added. [$Pd(PPh_2)Cl_2$] (36 mg, 0.05 mmol) was added under $N_2$ and then the reaction mixture was heated at 50 °C for 36 h. The crude product was extracted with DCM followed by brine wash and dried over $MgSO_4$. The resulting solutions were concentrated by rotary evaporator, and purified by column chromatography, (hexane:ethyl acetate 7:3) to give a light yellow solid. (0.60 g, yield 60%). $^1$H NMR (300 MHz, $CDCl_3$, $\delta$): 9.04 (br, 2H), 8.04 (m, 2H), 7.69 (s, 1H), 7.54 (s, 1H), 7.32 (m, 2H), 6.0 (s, 2H), 4.48 (m, 1H), 4.06 (t, $J$ = 6.0 Hz, 4H), 2.20 (m, 2H), 1.97 (m, 2H), 1.77 (m, 4H), 1.64 (m, 4H), 1.36–1.52 (m, 10H), 1.42–0.92 (m, 14H), 0.80 (t, $J$ = 6.9 Hz, 6H), 0.71 (t, $J$ = 6.2, 6H). $^{13}$C NMR (75 MHz, $CDCl_3$, $\delta$): 161.50, 156.79, 149.67, 137.77, 122.65, 121.97, 120.45, 114.39, 111.98, 105.50, 100.79, 79.45, 56.26, 45.75, 32.75, 30.50, 30.45, 29.27, 28.67, 27.96, 27.82, 25.78, 25.49, 21.57, 21.44, 12.96; EIMS [$M^+$] calcd. $m/z$ = 786.06, found 787.0. Anal. Calcd. For $C_{49}H_{62}N_4O_4$: C, 74.87; H, 8.08; N, 8.91; O, 8.14; found: C, 74.68; H, 7.97; N, 8.77.

### 2.4.9. 6,6′-(9,9-Dihexyl-9H-fluorene-2,7-diyl)bis(ethyne-2,1-diyl) bis(1-hexylpyrimidine-2,4(1H,3H)-dione) (**F**)

The synthesis procedure for **F** was followed using the same procedure as that of **C**. After purification (hexane:ethyl acetate 7:3) afforded a light yellow solid. (0.58 g, yield 58%). $^1$H NMR (300 MHz, $CDCl_3$, $\delta$): 9.60 (br, 2H), 7.77 (d, $J$ = 8.1 Hz, 2H), 7.53 (m, 4H), 6.04 (m, 2H) 4.01 (t, $J$ = 7.8 Hz, 4H), 2.0 (t, $J$ = 8.1 Hz, 4H), 1.82 (t, $J$ = 7.2 Hz, 4H), 1.44–1.34 (m, 12H), 1.36–1.08 (m, 12H), 1.15–1.08 (m, 12H), 0.88 (t, $J$ = 6.9 Hz, 6H), 0.77 (t, $J$ = 7.2, 6H), 0.59 (m, 4H). $^{13}$C NMR (75 MHz, $CDCl_3$, $\delta$): 162.96, 151.95, 151.08, 142.41, 138.89, 131.72, 126.58, 121.05, 119.76, 106.89, 101.28, 81.30, 55.84, 46.94, 40.31, 31.67, 29.77, 29.02, 26.65, 23.97, 22.77, 22.75, 14.19; EIMS [$M^+$]

calcd. m/z = 771.04, found 772.0. Anal. Calcd. For $C_{49}H_{62}N_4O_4$: C, 76.33; H, 8.10; N, 7.27; O, 8.30; found: C, 76.00; H, 7.97; N, 7.17.

### 2.5. Synthesis of *PBTH* via stille coupling polymerization

Into a 25 ml two-neck flask, 1 equiv. of dibromo monomers (**M1** and **M3**) and 2 equiv. of 2,6-bis(tributylstannyl)-4-(tridecan-7-yl)-4*H*-dithieno[3,2-b:2′,3′-d]pyrrole (**M2**) were added in anhydrous toluene and deoxygenated with nitrogen for 30 min. The $Pd(PPh_3)_4$ (1 mol %), was transferred into the mixture in a dry environment. The reaction mixture was stirred at 110 °C for 48 h, and then an excess amount of 2-bromothiophene was added to end-cap the trimethylstannyl groups for 4 h. After cooling to room temperature, the solution was added dropwise into MeOH (200 ml). The crude polymer was collected, dissolved in hot $CHCl_3$, filtered through a 0.5-μm poly(tetrafluoroethylene) (PTFE) filter, and reprecipitated in MeOH. The solid was washed with acetone, hexane, and $CHCl_3$ in a Soxhlet apparatus. The $CHCl_3$ solution was concentrated and then added dropwise into MeOH. Finally, the product was collected and dried under vacuum to give polymer **PBTH** (140 mg, 77%) with $M_w$ = 21,100 g/mol and polydispersity index (PDI) = 1.65. $^1$H NMR (300 MHz, $CDCl_3$): δ 7.17 (m), 7.21–7.15 (m), 4.91 (br), 4.21 (m), 3.56 (br, 2H), 2.99 (m), 2.11–1.74 (m), 1.27–1.49 (m), 1.66–1.11 (m), 0.91–0.81 (m). Anal. Calcd For: $C_{91}H_{118}N_{10}S_8$: C, 67.95; H, 7.39; N, 8.71; S, 15.95; Found: C, 66.38; H, 7.85; N, 8.12.

### 2.6. Preparation of supramolecular polymer networks (*PBTH/C* and *PBTH/F*)

Supramolecular polymer networks (**PBTH/C** and **PBTH/F**) were prepared by dissolving 2 mol of polymer (**PBTH**) and 1 mol of bi-functional conjugated cross-linker (**C** and **F**) in minimum amounts of $CHCl_3$ and then the solvent was evaporated under ambient temperature.

## 3. Results and discussion

### 3.1. Synthesis and characterization

The synthetic details of monomer **M1**, π-conjugated cross-linkers (**C** and **F**), and conjugated main-chain polymer **PBTH** are outlined in Scheme 1. 4,6-Dichloro-*N*,*N*-diphenyl-1,3,5-triazin-2-amine (**1**) was prepared by reacting of diphenylamine and 2,4,6-trichloro-1,3,5-triazine, and subsequently converted to $N^2$,$N^4$-dibutyl-$N^6$,$N^6$-diphenyl-1,3,5-triazine-2,4,6-triamine (**2**) and Finally brominated to **M1** by NBS at 0–5 °C. 1-Hexyluracil (**3**) was prepared by reaction of unsubstituted uracil with 1-bromohexane in the presence of $K_2CO_3$ and DMSO. Deprotonation of compound **3** with LDA and addition of $I_2$ could yield 1-hexyl-6-iodouracil (**4**). Then, 2,7-dibromo-9-(tridecan-7-yl)-9*H*-carbazole [11a] (**5**) was reacted with 3-methyl-1-butyn-3-ol via the Sonogashira coupling reaction to form 4,4′-(9-(tridecan-7-yl)-9*H*-carbazole-2,7-diyl)bis(2-methylbut-3-yn-2-ol) (**6**) and further deprotected by refluxing 2-propanol in a basic condition to obtain 2,7-diethynyl-9-(tridecan-7-yl)-9*H*-carbazole (**7**). The H-bonded cross-linkers **C** and **F** were synthesized via palladium catalyzed Sonogashira cross-coupling reactions of compound **4** with compound **7** and 2,7-diethynyl-9,9-dihexyl-9*H*-fluorene (**8**), respectively. In addition, compounds **8** [6a], **M2** [17], and **M3** [11a] were prepared by similar procedures reported earlier. In this study, a conjugated main-chain polymer (**PBTH**) consisting of DTP and **M1** units as the electron-donating moieties and bithiazole unit as the electron-accepting moiety (sandwiched between two thiophene units) were synthesized by Pd(0)-catalyzed Stille coupling polymerization in toluene at 110 °C with an input molar ratio of m:*n* = 1:1 (output molar ratio of m:*n* = 1.32:1 determined by NMR characterization). The chemical structures of **PBTH**, **M1**, **C** and **F** were satisfactorily characterized by $^1$H NMR, MS spectroscopy, and elemental analyses. The weight average molecular weight ($M_w$) of **PBTH** was determined by gel permeation chromatography (GPC) with THF as the eluting solvent and polystyrene as a standard. The $M_w$ and polydispersity index (PDI) of **PBTH** were found to be 21,100 g/mol and 1.65, respectively. The decomposition temperatures with 5% weight loss ($T_d$) of polymer **PBTH** and supramolecular polymer networks **PBTH/C** and **PBTH/F** were measured by thermogravimetric analysis (TGA) (see Fig. 2) and found to be 380, 402, and 391 °C, respectively, indicating supramolecular polymer networks **PBTH/C** and **PBTH/F** have better thermal stabilities than polymer **PBTH**. These thermal stabilities are adequate for their applications in polymer solar cells and other optoelectronic devices.

### 3.2. IR measurements

The existence of multiple H-bonds in the H-bonded complexes can be confirmed by FT-IR spectroscopy. Therefore, IR spectra of π-conjugated cross-linkers **C** and **F**, conjugated main-chain polymer **PBTH**, and supramolecular polymer networks **PBTH/C** and **PBTH/F** are shown in Fig. 3. Both IR spectra of cross-linkers **C** and **F** are located likewise at 1702–1704 $cm^{-1}$ and 3145–3147 $cm^{-1}$ for free C═O and N–H stretching bands, respectively [13,18]. The peak at 3280 $cm^{-1}$ can be assigned to stretching frequency of amine groups (–NH–) present in **PBTH**. Therefore, the C═O stretching bands of supramolecular polymer networks **PBTH/C** and **PBTH/F** were considerably shifted to lower wave numbers of 1683 and 1680 $cm^{-1}$, respectively, and the –NH– stretching bands were significantly shifted to higher wave numbers of 3310 and 3305 $cm^{-1}$, respectively. Consequently, the large shifts of wave numbers in C═O and N–H stretching bands during the formation of supramolecular polymer networks (**PBTH/C** and **PBTH/F**) indicate the presence of multiple H-bonds between polymer **PBTH** and cross-linkers (**C** and **F**) [13a,19].

### 3.3. Optical properties

The UV–visible absorption spectra of a conjugated main-chain polymer **PBTH**, π-conjugated cross-linkers **C** and **F** (in dichlorobenzene solutions and solid films), and supramolecular polymer networks **PBTH/C** and **PBTH/F** (in solid films only) are shown in Fig. 4, and their photophysical properties are summarized in Table 1. As shown in Fig. 4b, the light harvesting capability of **PBTH** can be directly tuned by forming multiple H-bonds with π-conjugated cross-linkers **C** and **F**, which could be clearly identified from their absorption spectra of supramolecular polymer networks **PBTH/C** and **PBTH/F** in solid films. The absorption maxima of π-conjugated cross-linkers **C** and **F** in dichlorobenzene solutions are 379 and 369 nm, respectively, and in solid films are 419 and 409 nm, respectively. Because of the inter-chain association and π-π stacking, the absorption wavelengths of π-conjugated cross-linkers **C** and **F** in solids films generally show red-shifts of 40 and 30 nm, respectively, in contrast to those in dilute solutions [15]. The absorption maxima of **PBTH** in the dichlorobenzene solution and solid film are found to be 523 and 535 nm, respectively, which can be attributed to the intramolecular charge transfer (ICT) from the donor to acceptor moieties [11]. In solid films, UV–visible spectra of supramolecular polymer networks **PBTH/C** and **PBTH/F** are found to be 550 and 544 nm, respectively, and red shifted about 15 and 9 nm (from **PBTH**), respectively, due to the enhanced π-π stacking and efficient charge transfer between polymer **PBTH** and cross-linkers (**C** and **F**) [19b,20]. New peaks of 407 and 396 nm were formed in the visible region of **PBTH/C** and **PBTH/F**, respectively, which are mainly attributed to the cross-linkers (**C** and **F**) and help **PBTH/C** and **PBTH/F** to harvest sufficient amounts of lights from the

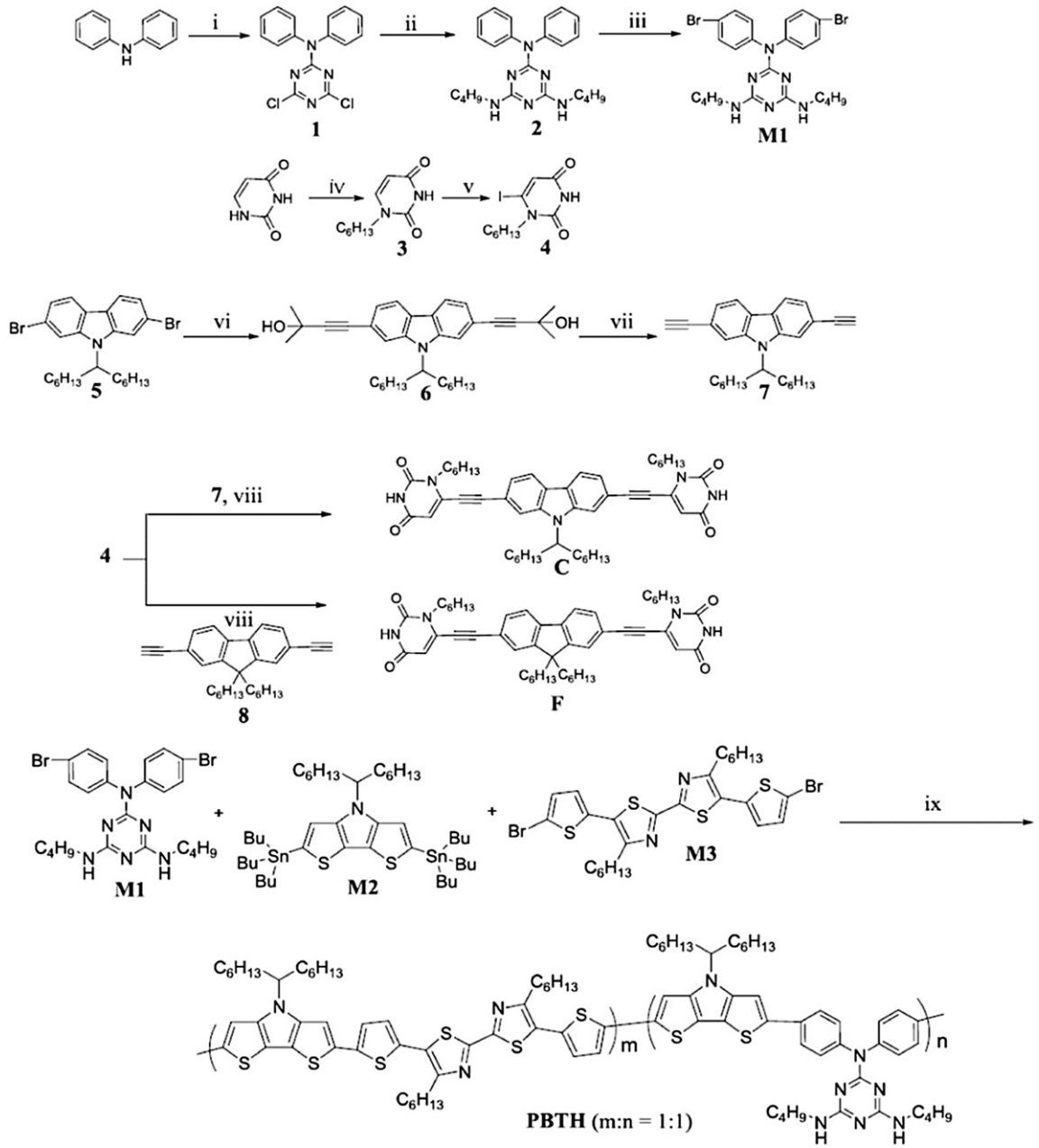


**Scheme 1.** Synthesis routes of monomer **M1**, **C**, **F**, and polymer **PBTH**. Reagents and conditions: (i) diisopropylethylamine, THF, 2,4,6-trichloro-1,3,5-triazine, 20 °C, 3 h; (ii) sodium bicarbonate, bromobutane,1,4-dioxane, reflux, overnight; (iii) NBS, 0–5 °C, THF; (iv) $K_2CO_3$, DMSO, 45 °C, overnight; (v) −78 °C, LDA, THF, 5 h, $I_2$; (vi) THF/$Et_3N$ (1/1), 3-methyl-1-butyn-3-ol, $Pd(PPh_3)_2Cl_2$, $PPh_3$, CuI, 12 h; (vi) KOH, 2-propanol, 4 h; (viii) $Ph_3P$, CuI, THF, $Et_3N$, $Pd(PPh_2)Cl_2$, 50 °C, overnight; (ix) Toluene, $Pd(PPh_3)_4$, 110 °C, 48 h.

visible region and further to improve the performance of photovoltaic devices [21].

As shown in Table 2, the optical band gaps ($E_g^{opt}$) of the polymers in solid films determined by the cut off wavelengths of the optical absorptions are in the range of 1.72–1.81 eV. Therefore, this result implies that it is an efficient way to design supramolecular polymer networks to absorb maximum photons from the visible region for enhanced photovoltaic applications.

### 3.4. Electrochemical properties

To investigate the redox behavior of polymer (**PBTH**) and supramolecular polymer networks (**PBTH/C** and **PBTH/F**) and their electronic states, i.e., the highest occupied molecular orbital (HOMO) and lowest unoccupied molecular orbital (LUMO) levels, the electrochemical properties of polymers were investigated by cyclic voltammetry (CV) measurements on polymer films in acetonitrile containing 0.1 M tetrabutylammonium hexafluorophosphate ($Bu_4NPF_6$) at a potential scanning rate of 100 mV/s. The oxidation and reduction cyclic voltammograms of all polymers are shown in Fig. 5, and their electrochemical properties, such as the onset oxidation potentials ($E_{ox}^{onset}$), HOMO and LUMO levels of polymers, are summarized in Table 1. It can be seen that all polymers **PBTH**, **PBTH/C**, and **PBTH/F** possessed three oxidation and one reduction irreversible peaks, and π-conjugated cross-linkers **C** and **F** possessed one oxidation and reduction irreversible peaks at positive and negative potentials. The $E_{ox}^{onset}$ values were found to be 0.55, 0.66, 0.68, 1.26, and 1.49 V for **PBTH**, **PBTH/C**, **PBTH/F**, **C**, and **F,**

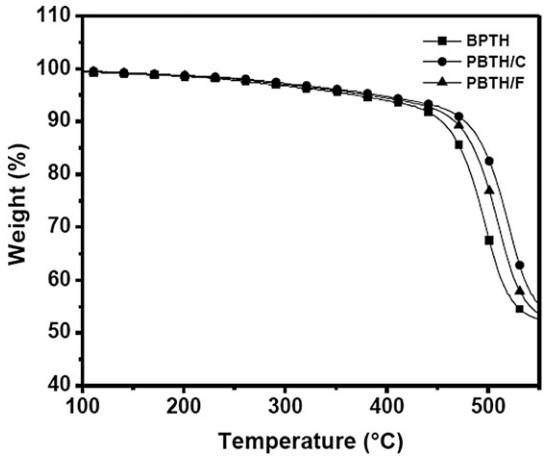


**Fig. 2.** TGA plots of polymer **PBTH** and supramolecular polymer networks (**PBTH/C**, and **PBTH/F**) with a heating rate of 10 °C/min under $N_2$.

respectively. The HOMO energy levels were estimated by the oxidation potentials from the reference energy level of ferrocene according to the following equation

$$E_{\mathrm{HOMO}} = \left[ -\left( E_{\mathrm{ox}} - E_{\mathrm{onset(FC/FC+\ VS.\ Ag/Ag+)}} \right) - 4.8 \right] \mathrm{eV}$$

Where 4.8 eV is the energy level of ferrocene below the vacuum level and $E_{\mathrm{onset(FC/FC+\ VS.\ Ag/Ag+)}} = 0.45$ eV and $E_{\mathrm{ox}}$ is the oxidation potential of each polymer [22]. The HOMO levels of polymer **PBTH**, supramolecular polymer networks (**PBTH/C** and **PBTH/F**), and π-conjugated cross-linkers (**C** and **F**) were found to be −4.90, −5.01, −5.03, −5.61, and −5.84 eV, respectively. Obviously, the supramolecular incorporation of electron rich building blocks, such as carbazole and fluorene units, enhanced oxidation potentials of **PBTH/C** and **PBTH/F** and lowered the HOMO levels due to their lower HOMO energy levels [23]. The LUMO levels of **PBTH**, **PBTH/C**, **PBTH/F**, **C** and **F** were obtained from their optical band gaps, and the HOMO energy levels were calculated by using the following equation [24].

$$E_{\mathrm{LUMO}} = E_{\mathrm{HOMO}} + E_{\mathrm{g}}^{opt}$$

The LUMO energy levels were found to be −3.09, −3.29, −3.28, −3.03, and −3.18 eV for **PBTH**, **PBTH/C**, **PBTH/F**, **C**, and **F**

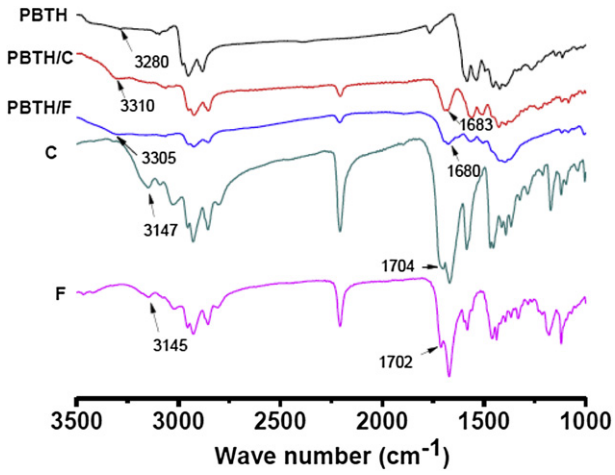


**Fig. 3.** FT-IR spectra of polymer **PBTH**, supramolecular polymer networks (**PBTH/C** and **PBTH/F**) and cross-linkers (**C** and **F**).

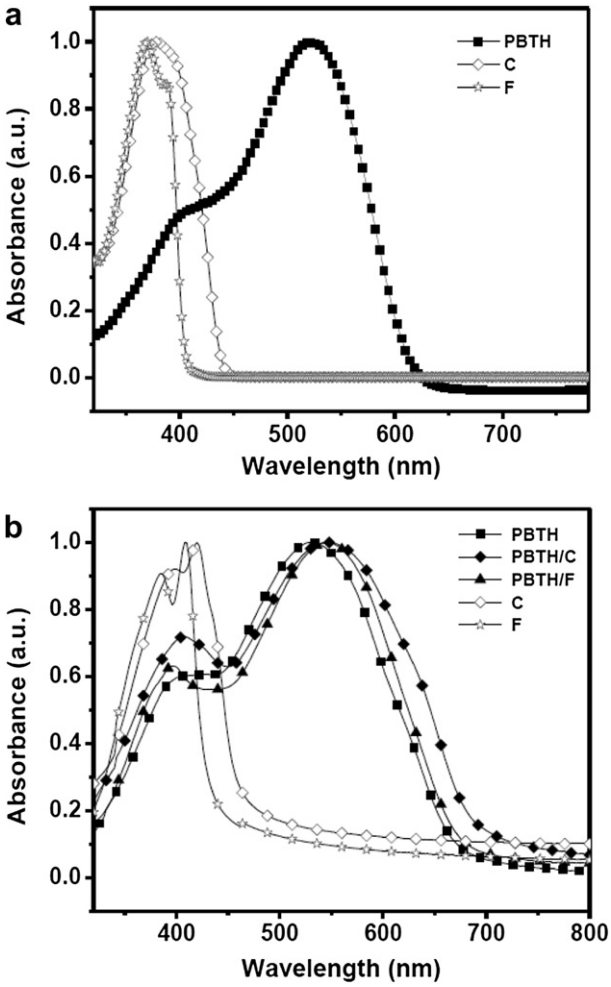


**Fig. 4.** Normalized UV–vis spectra of (a) polymer **PBTH** and conjugated cross-linkers **C** and **F** in dilute dichlorobenzene solutions and (b) supramolecular polymer networks **PBTH/C** and **PBTH/F** in solid films (on glass substrates).

respectively, and which depends on the strength of acceptors [11b]. The low HOMO levels of **PBTH/C** and **PBTH/F** from **PBTH** is an advantage for attaining high $V_{\mathrm{oc}}$ values in solar cell devices, because the $V_{\mathrm{oc}}$ value is directly proportional to the difference between the HOMO level of each donor polymer and the LUMO level of the acceptor derivative ($PC_{70}BM$) [25]. On the other hand, the LUMO energy level of the electron donor (polymer) has to be positioned above the LUMO energy level of $PC_{70}BM$ at least 0.3 eV, so the exciton binding energy of the polymer could be overcome and resulted in efficient electron transfer from donor to acceptor.

### 3.5. Photovoltaic properties

To investigate the photovoltaic properties of a conjugated main-chain polymer (**PBTH**) and supramolecular polymer networks (**PBTH/C** and **PBTH/F**) in PSC devices, the bulk heterojunction (BHJ) solar cell devices were fabricated by using polymers as electron donors and $PC_{70}BM$ as an electron acceptor with a device configuration of ITO/PEDOT:PSS(30 nm)/(copolymers):$PC_{70}BM$(1:1w/w) (~90 nm)/Ca(30 nm)/Al(100 nm). In order to obtain a better absorption coefficient in visible region, $PC_{70}BM$ was chosen as electron acceptor rather than $PC_{61}BM$ [25]. To achieve better performance in PSC devices, chlorobenzene was chosen as the solvent to obtain the blended polymer active layers with good film

**Table 1**
Optical and electrochemical properties of polymer **PBTH** and supramolecular polymer networks (**PBTH/C** and **PBTH/F**).

| Polymers | Solution[a] $\lambda_{abs}$ (nm) | Solid film[b] $\lambda_{abs}$ (nm) | $E_g^{opt}$ (eV) | $E_{ox}^{onset}$ (V) | $E_{HOMO}$[c] (eV) | $E_{LOMO}$[d] (eV) |
|---|---|---|---|---|---|---|
| **C** | 379 | 419 | 2.58 | 1.26 | −5.61 | −3.03 |
| **F** | 369 | 409 | 2.66 | 1.49 | −5.84 | −3.18 |
| **PBTH** | 523 | 535 | 1.81 | 0.55 | −4.90 | −3.09 |
| **PBTH/C** | – | 407, 550 | 1.72 | 0.66 | −5.01 | −3.29 |
| **PBTH/F** | – | 396, 544 | 1.75 | 0.68 | −5.03 | −3.28 |

[a] In dichlorobenzene.
[b] Spin coated from dilute dichlorobenzene solution on glass surface.
[c] HOMO $= [-(E_{onset} - E_{onset(FC/FC+\ vs.\ Ag/Ag+)}) - 4.8]$ eV where 4.8 eV is the energy level of ferrocene below the vacuum level and $E_{onset(FC/FC+\ vs.\ Ag/Ag+)} = 0.45$ eV.
[d] $E_{LUMO} = E_{HOMO} + E_g^{opt}$.

**Table 2**
Photovoltaic properties of polymer **PBTH** and supramolecular polymer networks (**PBTH/C** and **PBTH/F**).

| Weight ratio of polymer to $PC_{70}BM$ | $V_{oc}$ (V) | $J_{sc}$ (mA/cm$^2$) | FF | PCE (%) |
|---|---|---|---|---|
| **PBTH**: $PC_{70}BM = 1:1$ | 0.51 | 2.73 | 0.36 | 0.52 |
| **PBTH/C**: $PC_{70}BM = 1:1$ | 0.60 | 4.58 | 0.35 | 0.97 |
| **PBTH/C**: $PC_{70}BM = 1:2$ | 0.60 | 7.16 | 0.36 | 1.56 |
| **PBTH/C**: $PC_{70}BM = 1:3$ | 0.58 | 4.97 | 0.30 | 0.87 |
| **PBTH/F**: $PC_{70}BM = 1:1$ | 0.60 | 3.28 | 0.35 | 0.68 |
| **PBTH/F**: $PC_{70}BM = 1:2$ | 0.61 | 3.66 | 0.36 | 0.80 |
| **PBTH/F**: $PC_{70}BM = 1:3$ | 0.58 | 3.09 | 0.32 | 0.57 |

qualities. Fig. 6 shows the *J-V* curves of polymer solar cell (PSC) devices under the condition of AM 1.5 at 100 mW/cm$^2$, and the open circuit voltage ($V_{oc}$), short-circuit current density ($J_{sc}$), fill factor (FF), and power conversion efficiency (PCE) values are summarized in Table 2.

The obtained PCE value of conjugated main-chain polymer **PBTH** was found to be 0.52% with $V_{oc} = 0.51$ V, $J_{sc} = 2.81$ mA/cm$^2$, and FF = 0.36. However, a similar alternating copolymer reported by Li et al., which consisted of DTP and **M3** units, only achieved a lower PCE value of 0.06% and a $V_{oc}$ of 0.26 V. In addition, a polymer similar to **PBTH** was reported to possess a PCE value of 0.69% and a $V_{oc}$ value of 0.40 V [11c]. The lower $V_{oc}$ value (0.51 V) of polymer **PBTH** was because of its higher HOMO level (−4.90 eV),

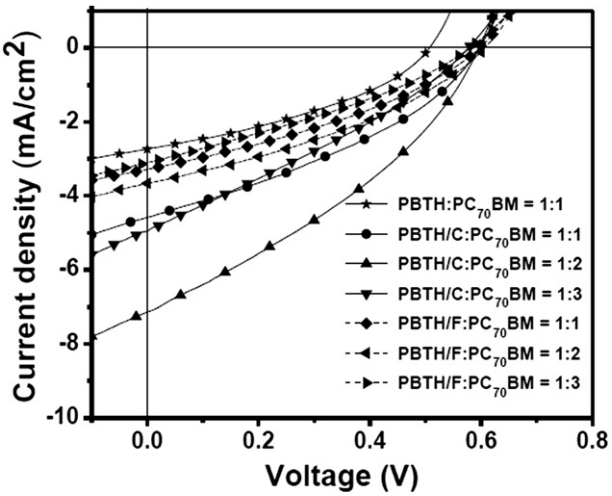


**Fig. 6.** *J–V* characteristics of **PBTH**, **PBTH/C**, and **PBTH/F** under illumination of AM 1.5 at 100 mW/cm$^2$.

whereas its supramolecular polymer networks **PBTH/C** and **PBTH/F** showed improved $V_{oc}$ values (0.60 and 0.61 V, respectively) due to of their lower HOMO levels (−5.01 and −5.03 eV, respectively) by the supramolecular design. The PCE values of PSC devices containing **PBTH/C** and **PBTH/F** with $PC_{70}BM$ in a weight ratio of 1:1 were found to be 0.97% and 0.68%, respectively. Hence, both supramolecular polymer networks **PBTH/C** and **PBTH/F** showed improved $J_{sc}$ values owing to the enhanced crystallinities compared with **PBTH**, which can be further verified by the powder X-ray diffraction (XRD) patterns. As demonstrated in Fig. 7, the XRD patterns of polymer (**PBTH**) and supramolecular polymer networks (**PBTH/C** and **PBTH/F**) were analyzed. Compared with a single weak peak in the small angle region of polymer **PBTH**, both sharp peaks at the small angle region and broad peaks at the wide angle region were observed in supramolecular polymer networks **PBTH/C** and **PBTH/F.** Thus, the crystallinities of the supramolecular polymer networks **PBTH/C** and **PBTH/F** were much improved due to the presence of multiple hydrogen bonds, which enhanced the chain-reorganization and self-assembled behavior and thus to induce higher PCE values of H-bonded polymer network (**PBTH/C** and **PBTH/F**) [1a,3a,22].

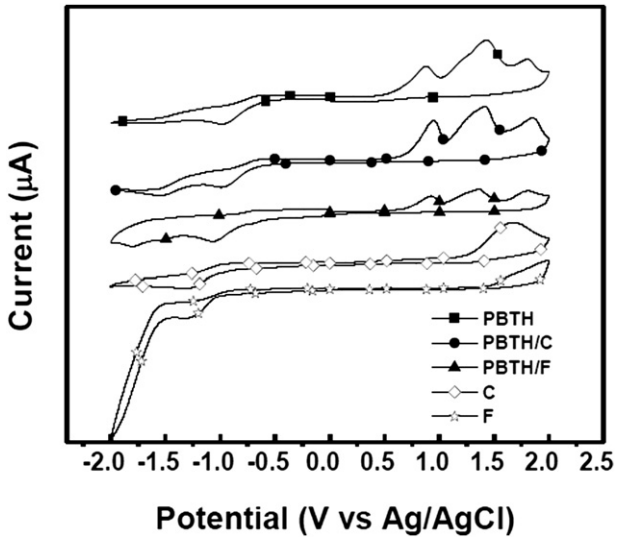


**Fig. 5.** Cyclic voltammograms of **PBTH**, **C**, **F**, **PBTH/C**, and **PBTH/F** in solid films at a scan rate of 100 mV/s.

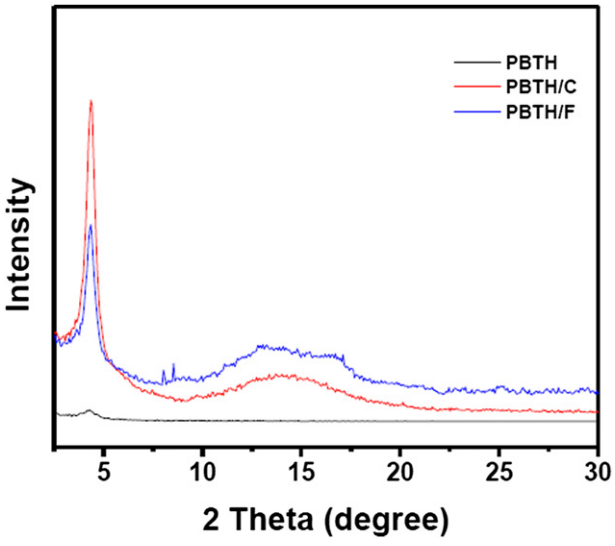


**Fig. 7.** X-ray diffraction patterns of polymer **PBTH** and supramolecular polymer networks (**PBTH/C** and **PBTH/F**) in solid powders.

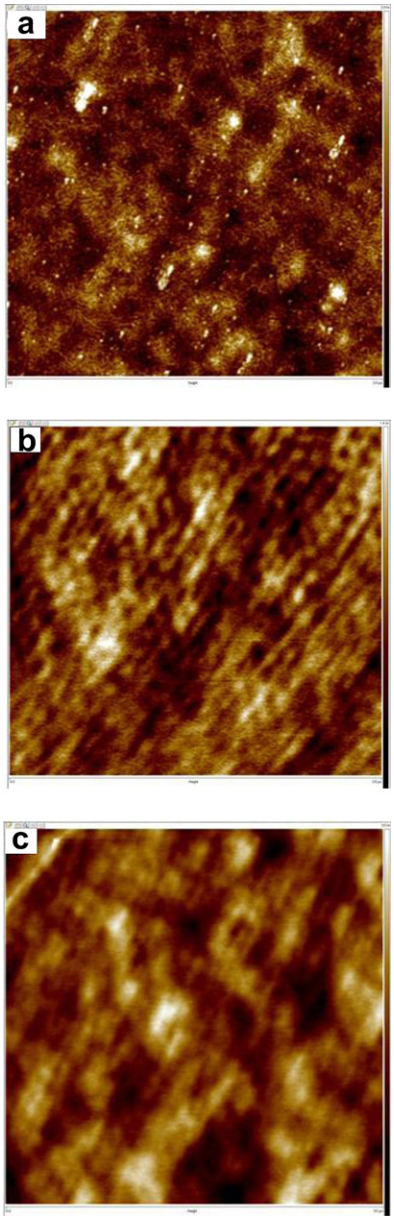


**Fig. 8.** AFM images of blended polymers with $PC_{70}BM$ in wt. ratios (a) PBTH: $PC_{70}BM$ (1:1), (b) PBTH/C: $PC_{70}BM$ (1:2), and (c) PBTH/F: $PC_{70}BM$ (1:2).

The photovoltaic properties of **PBTH**, **PBTH/C**, and **PBTH/F** were investigated initially using a 1:1 weight ratio of polymer:$PC_{70}BM$, then different blending ratios of polymer:$PC_{70}BM$ were applied to optimize their PCE values of **PBTH/C** and **PBTH/F**. As illustrated in Table 2, the maximum PCE values of 1.56% and 0.80% were obtained in the PSC devices containing **PBTH/C** and **BPTH/F**, respectively, with a weight ratio of polymer:$PC_{70}BM$ = 1:2, where the photovoltaic properties of **PBTH/C** with the optimum PCE value (1.56%) possessed $V_{oc}$ = 0.60 V, $J_{sc}$ = 7.16 mA/cm$^2$, and FF = 0.36. Indeed, the weight ratios between polymer donors and $PC_{70}BM$ acceptor played a key role in the PCE values of all PSC devices [17,26]. However, by increasing the weight ratios of $PC_{70}BM$ in supramolecular polymer networks **PBTH/C** or **PBTH/F** (i.e., polymer:$PC_{70}BM$ = 1:3 w/w), both $J_{sc}$ and PCE values were reduced (see Table 2), which might be attributed to the reduced interfacial area of exciton dissociation and the insufficient percolation for charge transport in blended films [11a,17,27].

The surface morphology of the active layer in solar cell devices is also a key parameter for the device performance [28]. AFM images of blended polymers **PBTH**, **PBTH/C**, and **PBTH/F** mixed with $PC_{70}BM$ in wt. ratios of 1:1, 1:2, and 1:2, respectively, are presented in Fig. 8 and their root-mean-square roughness ($R_{rms}$) values were found to be 0.93, 0.40, and 0.85 nm, respectively. All the active layers of **PBTH**, **PBTH/C**, and **PBTH/F** showed good film formation to have smooth surfaces with no obvious aggregations (only nano-scale phase separations) between polymers and $PC_{70}BM$. A higher $R_{rms}$ value found at **PBTH** blended with $PC_{70}BM$ in a wt. ratio of 1:1 compared with supramolecular polymer networks **PBTH/C** and **PBTH/F** blended with $PC_{70}BM$ in a wt. ratio of 1:2. This larger $R_{rms}$ value of **PBTH** blended with $PC_{70}BM$ resulted in the decreased diffusional escape probabilities for mobile charge carriers, and hence increased their recombinations [29]. Therefore, less aggregations between supramolecular networks **PBTH/C** and **PBTH/F** and $PC_{70}BM$ allows for better photogenerated charges and inducing higher $J_{sc}$ values via supramolecular engineering of solar cell devices.

Interestingly, compared with polymer **PBTH** (with $V_{oc}$ = 0.51 V), the $V_{oc}$ value of the solar cell devices containing supramolecular polymer networks **PBTH/C** and **PBTH/F** (as polymer:$PC_{70}BM$ = 1:1 w/w) increased to 0.60 V. The supramolecular design resulting in an increase of 0.09 V in $V_{oc}$ is a good agreement with the HOMO levels (see Table 1) of −4.9, −5.01, and −5.03 eV for **PBTH**, **PBTH/C**, and **PBTH/F**, respectively [27]. Various parameters improved in the suramolecular design, such as more efficient light harvests, lower HOMO energy levels, and higher crystallinities, are responsible for the enhancement of $V_{oc}$ and $J_{sc}$ values in PSC devices containing supramolecular polymer networks **PBTH/C** and **PBTH/F** in contrast to polymer **PBTH**. The enhanced photovoltaic properties of supramolecular polymer networks **PBTH/C** and **PBTH/F** indicate that the supramolecular approach is one of an ideal design for high-performance donor-acceptor polymer solar cells.

## 4. Conclusions

In summary, we have developed novel supramolecular polymer networks **PBTH/C** and **PBTH/F** based on the formation of multiple hydrogen bonds between conjugated main-chain polymer **PBTH** and uracil-based conjugated cross-linkers **C** and **F** (in proper molar amounts) through complementary melamine and uracil moieties. The supramolecular formation of multiple hydrogen bonds successfully characterizated by IR, and UV–Vis spectra measurements. The supramolecular concept has been successfully applied to tune the photophysical, electrochemical, and photovoltaic properties of supramolecular polymer networks **PBTH/C** and **PBTH/F** compared with polymer **PBTH**. The power conversion efficiencies (PCE) values of PSC devices containing supramolecular polymer networks **PBTH/C** and **PBTH/F** (as polymer:$PC_{70}BM$ = 1:1 w/w) are found to be 0.97 and 0.68%, respectively, in contrast to 0.52% for polymer **PBTH**. The optimum photovoltaic performance with the highest PCE value of 1.56% was obtained in the PSC device containing supramolecular polymer networks **PBTH/C** as polymer:$PC_{70}BM$ = 1:2 w/w. This supramolecular design is a encouraging approach on the further improvements of any most excellent donor-acceptor photovoltaic polymers to be in conjunction with efficient conjugated cross-linkers complementarily through supramolecular interactions for future polymer solar cell applications.

## Acknowledgements

We acknowledge the financial supports from the National Science Council of Taiwan (ROC) through NSC 99-2113-M-009-006-MY2 and National Chiao Tung University through 97W807.

## References


[1] (a) Greef TFAD, Smulders MMJ, Wolffs M, Schenning APHJ, Sijbesma RP, Meijer EW. Chem Rev 2009;109:5687–754;
(b) Lianes-Pallas A, Palma CA, Piot L, Belbakra A, Listorti A, Prato DM, et al. J Am Chem Soc 2009;131:509–20;
(c) González-Rodrıáguez D, Schenning APHJ. Chem Mater 2011;23:310–25.

[2] (a) Shunmugam R, Gabriel GJ, Amaer KA, Tew GN. Macromol Rapid Commun 2010;31:784–93;
(b) Yan P, Chowdhury A, Holman MW, Adams DM. J Phys Chem B 2005;109:724–30.

[3] (a) Ishida K, Weibel V, Yoshie N. Polymer 2011;52:2877–82;
(b) Kuo SW, Lin CT, Chen JK, Ko FH, Chang FC, Jeong KU. Polymer 2011;52:2600–8.

[4] (a) Würthner F, Chen Z, Hoeben FJM, Osswald P, You CC, Jonkheijm P, et al. J Am Chem Soc 2004;126:10611–8;
(b) Song M, Park JS, Yoon KJ, Kim CH, Im MJ, Kim JS, et al. Org Electronics 2010;11:969–78.

[5] (a) Yang B, Li G, Zhang X, Shu X, Wang A, Zhu X, et al. Polymer 2011;52:2537–41;
(b) Chen HW, Lin TP, Chang FC. Polymer 2002;43:5281–8.

[6] (a) Chen YY, Tao YT, Lin HC. Macromolecules 2006;39:8559–66;
(b) Padhy H, Sahu D, Chiang IH, Patra D, Kekuda D, Chu CW, et al. J Mater Chem 2011;21:1196–205;
(c) Tao Y, Xu Q, Li N, Lu J, Wang L, Xia X. Polymer 2011;52:4661–7.

[7] (a) Gendron D, Leclerc M. Energy Environ Sci 2011;4:1225–37;
(b) Boudreault PLT, Najari A, Leclerc M. Chem Mater 2011;23:456–69;
(c) Wang E, Wang M, Wang L, Duan C, Zhang J, Cai W, et al. Macromolecules 2009;42:4410–5.

[8] (a) Price SC, Stuart AC, Yang L, Zhou H, You W. J Am Chem Soc 2011;133:4625–31;
(b) Zhou H, Yang L, Stuart AC, Price SC, Liu S, You W. Angew Chem Int Ed 2011;50:2995–8.

[9] (a) Yue W, Zhao Y, Shao S, Tian H, Xie Z, Geng Y, et al. J Mater Chem 2009;19:2199–206;
(b) Zhang M, Fan H, Guo X, He Y, Zhang Z, Min J, et al. Macromolecules 2010;43:5706–12;
(c) Zhang M, Fan H, Guo X, Yang Y, Wang S, Zhang ZG, et al. J Polym Sci Part A Polym Chem 2011;49:2746–54.

[10] (a) Chen L, Deng D, Nan Y, Shi M, Chan PKL, Chen H. J Phys Chem C 2011;115:11282–92;
(b) Patra D, Sahu D, Padhy H, Kekuda D, Chu CW, Wei KH, et al. Macromol Chem Phys 2011;212:1960–70.

[11] (a) Patra D, Sahu D, Padhy H, Kekuda D, Chu CW, Wei KH, et al. J Polym Sci Part A Polym Chem 2010;48:5479–89;
(b) Tamilavan V, Sakthivel P, Li Y, Song M, Kim CH, Jin SH. J Polym Sci Part A Polym Chem 2010;48:3169–77;
(c) Tamilavan V, Song M, Jin SH, Hyun MH. J Polym Sci Part A Polym Chem 2010;48:5514–21;
(d) He Y, Zhao G, Min J, Zhang M, Li Y. Polymer 2011;50:5505–8.

[12] Hoeben FJM, Zhang J, Lee CC, Pouderoijen MJ, Wolffs M, Würthner F, et al. Chem Eur J 2008;14:8579–89.

[13] (a) Piot L, Palma CA, Pallas AL, Prato M, Szekrényes Z, Kamarás K, et al. Adv Funct Mater 2009;19:1207–14;
(b) Yoosaf K, Belbakra A, Armaroli N, Llanes-Pallas A, Bonifazi D. Chem Commun 2009;46:2830–2.

[14] (a) El-ghayoury A, Schenning APHJ, Hal PAV, Duren JKJV, Janssen RAJ, Meijer EW. Angew Chem Int Ed 2001;40:3660–3;
(b) Jonkheijm P, Duren JKJV, Kemerink M, Janssen RAJ, Schenning APHJ, Meijer EW. Macromolecules 2006;39:784–8.

[15] (a) Huang JH, Velusamy M, Ho KC, Lin JT, Chu CW. J Mater Chem 2010;20:2820–5;
(b) Mazzio KA, Yuan M, Okamoto K, Luscombe CK. ACS Appl Mater Interfaces 2011;3:271–8.

[16] (a) Liang TC, Chiang IH, Yang PJ, Kekuda D, Chu CW, Lin HC. J Polym Sci Part A Polym Chem 2009;47:5998–6013;
(b) Sahu D, Padhy H, Patra D, Kekuda D, Chu CW, Chiang IH, et al. Polymer 2010;51:6182–92.

[17] Sahu D, Patra D, Padhy H, Huang JH, Chu CW, Lin HC. J Polym Sci Part A Polym Chem 2010;48:6182–92.

[18] Kuo CY, Su MS, Ku CS, Wang SM, Lee HY, Wei KH. J Mater Chem 2011;21:11605–12;
(b) Noro A, Ishihara K, Matsushita Y. Macromolecules 2011;44:6241–4.

[19] (a) Delbosc N, Reynes M, Dautel OJ, Wantz G, Lère-Porte JP, Moreau JJE. Chem Mater 2010;22:5258–70;
(b) Liu Y, Xiao S, Li H, Liu H, Lu F, Zhaung J, et al. J Phys Chem B 2004;108:6256–60.

[20] Yagai S, Kubota S, Unoike K, Karatsu T, Kitamura A. Chem Commun; 2008:4466–8.

[21] Khlyabich PP, Burkhart B, Ng CF, Thompson BC. Macromolecules 2011;44:5079–84.

[22] Li KC, Huang JH, Hsu YC, Huang PJ, Chu CW, Lin JT, et al. Macromolecules 2009;42:3681–93.

[23] (a) Wu JS, Cheng YJ, Dubosc M, Hsieh CH, Chang CY, Hsu CS. Chem Commun 2010;46:3259–61;
(b) Li W, Qin R, Yi Zhou Y, Andersson M, Li F, Zhang C, et al. Polymer 2010;51:3031–8;
(c) Inaganäs O, Zhang F, Andersson MR. Acc Chem Res 2009;4:1731–9.

[24] Zhang J, Cai W, Huang F, Wang E, Zhong C, Liu S, et al. Macromolecules 2011;44:894–901;
(b) Zhao W, Kai W, Xu R, Yang W, Gong X, Wu H, et al. Polymer 2010;51:3196–202.

[25] (a) Wang E, Ma Z, Zhang Z, Henriksson P, Inganäs O, Fengling Zhang F, et al. Chem Commun 2011;47:4908–10;
(b) Tamilavan V, Song M, Jin SH, Hyun MH. Polymer 2011;52:2384–90.

[26] Walker B, Tamayo AB, Dang X-D, Zalar P, Seo JH, Garcia A, et al. Adv Funct Mater 2009;19:3063–9.

[27] (a) Guo X, Xin H, Kim FS, Liyanage ADT, Jenekhe SA, Watson MD. Macromolecules 2011;44:269–77;
(b) Zhang G, Fu Y, Zhang Q, Xie Z. Polymer 2010;51:2313–9.

[28] (a) Patra D, Ramesh M, Sahu D, Padhy H, Chu CW, Wei KH, et al. J Polym Sci Part A Polym Chem; 2011. doi:10.1002/pola.25853;
(b) Zhang Y, Hau SK, Yip HL, Sun Y, Action O, Jen AKY. Chem Mater 2010;22:2696–8.

[29] Li Y, Li H, Xu B, Li Z, Chen F, Feng D, et al. Polymer 2010;51:1786–95.